Metallophysics and Advanced Technologies
Металофіз. новітні технол.
Metallofiz. Noveishie Tekhnol.
2026, vol. 48, No. 5, pp. 513–526
https://doi.org/10.15407/mfint.48.05.0513
Reprints available directly from the publisher

PACS numbers: 61.66.Fn, 61.72.Ff, 65.80.+n, 68.55.J-, 72.15.Jf, 73.50.Lw, 81.15.Cd

Formation of Manganese-Silicide Films by Magnetron Sputtering, Measurement of Crystal Structure, Thermoelectric and Electrophysical Parameters

K. T. Dovranov, M. T. Normuradov, I. R. Bekpulatov,
T. O. Buzrukov*, E. O. Davranov**, R. Yorkulov**, and I. Akbarov

Department of Physics, Karshi State University,
17 Kuchabag Str.,
180119 Karshi, Uzbekistan
**Termez University of Economics and Service,*
4b Farovon Str.,
190111 Termez, Uzbekistan
***University of Economics and Pedagogy,*
45 Do'stlik Str.,
Karshi, Uzbekistan

In this work, thin Mn_4Si_7 films are grown by the solid-state ion-plasma method using a magnetron-sputtering device, and their surface morphology, crystal structure, Miller indices, lattice parameters, thermoelectric and electrophysical parameters of the films are measured. Seebeck coefficient decreases, and finally, the sample is changed from *p*-type to *n*-type. Power factor turns out to be small ($P \cong 1$–4 mW/(m·K^2)) and increases very little in the temperature range of 300–450 K and increases sharply in the range of 500–580 K ($P \cong 850$–3690 mW/(m·K^2)). As the thickness decreases, the power factor increases. The band gap at room temperature for the sample prepared by the ion-plasma method is measured optically to be $E_g = 0.354$ eV. Studies show that Mn_4Si_7 layers with a size of ≤ 40 nm can be grown on the surface of the Si

Corresponding author: Quvondiq Dovranov
E-mail: quvondiqdavronm@gmail.com

Citation: K. T. Dovranov, M. T. Normuradov, I. R. Bekpulatov, T. O. Buzrukov, E. O. Davranov, R. Yorkulov, and I. Akbarov, Formation of Manganese-Silicide Films by Magnetron Sputtering, Measurement of Crystal Structure, Thermoelectric and Electrophysical Parameters, *Metallofiz. Noveishie Tekhnol.*, **48**, No. 5: 513–526 (2026). DOI: 10.15407/mfint.48.05.0513

crystal formed by the magnetron sputtering, but the Si crystal does not form a full-size Mn_4Si_7 layer. During thermal heating at 300–750 K, nanosize bubbles are observed to form in the thin Mn_4Si_7 coating grown under vacuum conditions; then, they are ruptured and the nanosize defects are formed. Then, at 750 K, the defects narrow down to form a single thin Mn_4Si_7 coating. The measurement results show that the thin films grown by the solid-state ion-plasma method are formed and their thermoelectric and electrophysical properties are improved.

Key words: Miller indices, interplanar distance, strict monocrystalline structure, Seebeck coefficient, power factor.

У даній роботі методою твердотільної йонної плазми з використанням пристрою магнетронного розпорошення вирощено тонкі плівки Mn_4Si_7 та виміряно морфологію їхньої поверхні, кристалічну структуру, Міллерові індекси, параметри ґратниці, термоелектричні й електрофізичні параметри плівок. Зеєбеків коефіцієнт зменшився, і зрештою тип зразків змінився з p-типу на n-тип. Коефіцієнт потужности виявився малим ($P \cong 1$–4 мВт/(м·К^2)) та дуже слабо збільшувався в діяпазоні температур 300–450 К і різко зростав у спостережуваному нами діяпазоні 500–580 К ($P \cong 850$–3690 мВт/(м·К^2)). Зі зменшенням товщини збільшується коефіцієнт потужности. Ширину забороненої зони за кімнатної температури для зразка, виготовленого йонно-плазмовою методою, було виміряно оптично, що становило $E_g = 0{,}354$ еВ. Дослідження показали, що шари Mn_4Si_7 розміром у ≤ 40 нм можуть бути вирощені на поверхні кристалу Si, утвореного магнетронним розпорошенням, але кристал Si не утворює повнорозмірний шар Mn_4Si_7. Під час термічного нагрівання за 300–750 К спостерігалося утворення нанорозмірних бульбашок у тонкому покритті Mn_4Si_7, вирощеному в умовах вакууму, а потім вони розривалися й утворювалися нанорозмірні дефекти. За 750 К дефекти звужуються, утворюючи єдине тонке покриття Mn_4Si_7. Результати мірянь свідчать про формування тонких плівок, вирощених методою твердотільної йонної плазми, та поліпшення їхніх термоелектричних і електрофізичних властивостей.

Ключові слова: Міллерові індекси, міжплощинна віддаль, чітка монокристалічна структура, Зеєбеків коефіцієнт, коефіцієнт потужности.

(Received 15 March, 2025; in final version, 2 July, 2025)

1. INTRODUCTION

High manganese silicide (HMS) is one of the promising materials for use in the field of silicon microelectronics [1]. Based on HMS films, it is possible to create infrared thermal radiation detectors. Detectors can record data into memory devices and measure fast processes associated with data transmission through various channels. In addition, it is possible to create light sources at significant wavelengths in the infrared range [2–4]. Therefore, studying the growth and electrical properties of HMS films is of great interest.

There is ion implantation, molecular beam epitaxial, ion plasma and chemical methods for producing thin films. Thin films obtained by the ion plasma method are practically not found in previously published literature, and this method can be called new. The ion plasma method was created by ionizing argon gases under high vacuum conditions.

Of all the silicon compounds that have thermoelectric efficiency, it is possible to select compounds that are of practical importance. These are, for example, solid solutions based on cobalt monosilicide (CoSi), higher manganese silicide ($MnSi_{1.7}$) and Mn_2X (X = Si, Ge, Sn). There is little data on the thermoelectric properties of Mn_4Si_7 materials [5, 6]. The high Seebeck coefficient, low resistance and high application temperature make them very attractive for power generation [7, 8]. However, the thermoelectric properties of n-type Mn_4Si_7 films have rarely been reported. We developed and characterized n-type polycrystalline Mn_4Si_7 thin films to understand the basic thermoelectric properties of the movie.

When preparing the sample, a ready-made Mn_4Si_7 target, heated and compacted, was used. Pure silicon with the crystal direction [111] was taken as a substrate. First, the silicon surface was cleaned of surface impurities using an 'ion gun' device in a vacuum. The purified sample was heated to 1720 K for 2 hours. Then, using argon gases under high vacuum conditions, 'ion plasma' was created from a manganese silicide target and thin films of Mn_4Si_7 of various thicknesses were obtained. The electrical conductivity and Seebeck coefficient of the resulting thin films were measured using a 'Netzch®SBA 458' measuring instrument.

Research shows that Mn_4Si_7 layers ≤ 40 nm in size can be grown on the surface of a Si crystal produced by magnetron sputtering, but the Si crystal does not form a full-size Mn_4Si_7 layer. During thermal heating at 300–750 K, the appearance of nanosize bubbles in a thin Mn_4Si_7 coating grown under vacuum conditions was observed; then, they burst and formed nanosize defects. Then, at a temperature of 750 K, the defects narrowed and formed a single thin Mn_4Si_7 coating (Fig. 1).

The surface morphology of Mn_4Si_7 crystals was studied under a microscope (Scios FEI, Quanta 200 3D). The surface morphology of Mn_4Si_7 was studied using an SPM 9700HT scanning probe microscope. For this purpose, a sample area measuring 500×500 nm was selected, lines were drawn on this area in one arbitrary direction, and the thickness of their full width was determined.

2. EXPERIMENTAL/THEORETICAL DETAILS

Polycrystalline HMS thin films were prepared using a magnetron sputtering system. A schematic diagram of the magnetron sputtering system used in this work is presented in Fig. 2. A high vacuum was created at a pressure of 10^{-6} Torr using a molecular turbo-pump (Pfeiffer

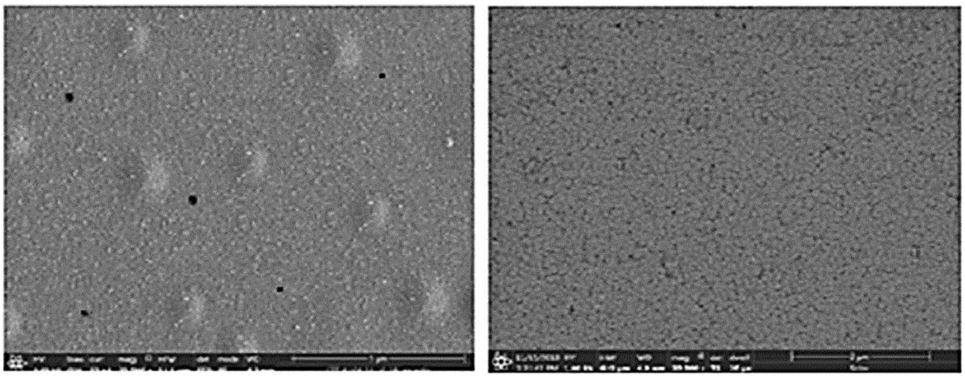

Fig. 1. Image of a thin Mn_4Si_7 film before and after heating to 300–750 K.

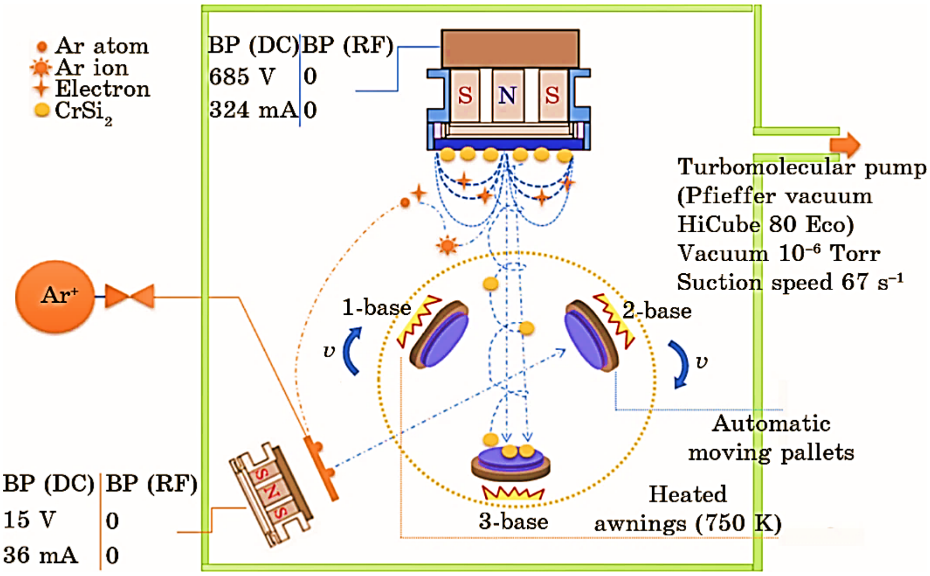

Fig. 2. Scheme of a magnetron-sputtering device.

vacuum) in the chamber of the Epos-PVD-Desk-Pro magnetron device for sputtering the Mn_4Si_7 target. First, the surface of the silicon wafers was mechanically cleaned with 20% dilute hydrofluoric acid, then the silicon surface was cleaned again by ionizing argon gas inside the chamber using an 'ion gun' treatment device installed in the chamber. A direct current source was used to sputter the Mn_4Si_7 target. The current in the magnetron power supply is of 657 mA, power is of 221 W, and voltage is of 336 V. The purity of the Mn_4Si_7 target is of 99.9%.

The deposition rate varies from 0.4 to 14 Å/s. The thickness of each layer was controlled on an 'SP307' monitor.

The electrical parameters of a thin layer of Mn_4Si_7 samples with a thickness of approximately 34.7–172 nm was studied on an ECOPIA instrument (HMS-5000). The surface morphology was analysed using atomic force microscopy. Structural analysis of the Mn_4Si_7 crystal was recorded on an XRD-6100 x-ray diffractometer; spectra were recorded at room temperature. Spectrogram peaks based on Miller indices and interplanar distances indicate newly formed manganese silicide compounds. The thermoelectric parameters of manganese silicide were measured using the 'SBA-458' measuring system. This setup allows you to measure the Seebeck coefficient and electrical conductivity as a function of temperature. The diagram of the measuring cell is shown in Fig. 3.

The sample is placed on the ceramic supports, inside of which microheaters are located. Two thermocouples and two current probes are connected to the bottom surface of the sample. Electrical conductivity is measured by the four-point method. This scheme allows current to flow through the sample in the forward and reverse directions. During the measurement, three current values are passed in each direction: I_{max}, $2I_{max}/3$, $I_{max}/3$. The value of I_{max} is selected based on the geometry and material of the sample. The program determines three current values, and applies each sample to the sample five times in the forward direction and five times in the opposite direction. Next, the voltage values U_A and U_B are measured between two positive and two negative thermocouple branches. Based on the measurements, a graph of voltage dependence on the missed current is plotted, and the electrical conductivity is calculated.

To measure the Seebeck coefficient using two microheaters inside the sample, a temperature gradient is created. After heating one side

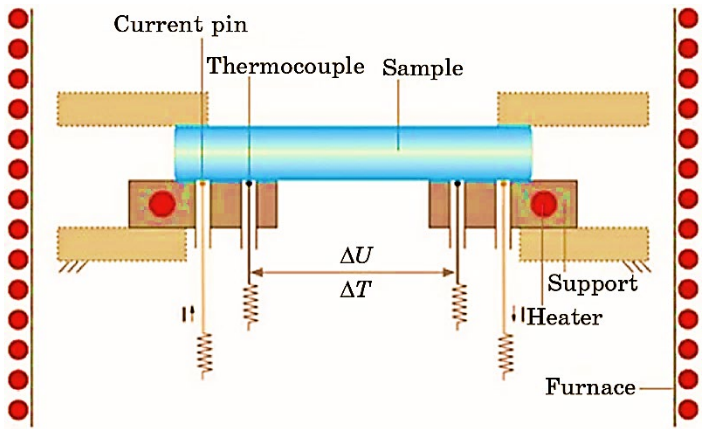

Fig. 3. Diagram of the SBA-458 Nemesis® measuring cell.

of the sample, it cools. Then, the other side of the sample is also heated and cooled. During this whole process, the values of the voltages U_A, U_B and U_{T1}, U_{T2} are measured. As for electrical conductivity, U_A and U_B are the voltages between the positive and negative branches of thermocouples. These values are measured concerning the temperature difference ΔT, which is the temperature gradient between the two sides of the sample. The value of ΔT is determined from the voltages U_{T1} and U_{T2}, coming from two thermocouples. Based on the measurement data, a graph of voltage versus temperature is plotted and the Seebeck coefficient is calculated. In this case, it is of ± 2 degrees from the point given by the operator.

The efficiency of thermoelectric materials is determined by a dimensionless quantity called the thermoelectric index [14]:

$$ZT = \sigma\alpha^2\tau/\lambda, \quad (1)$$

where σ is the electrical conductivity of the material, λ is the thermal conductivity, α is the Seebeck coefficient, and T is temperature. A material with $ZT = 1$ at room temperature is considered effective. As can be seen in formula (1), if there is the higher the quality factor, there is the higher the thermal conductivity and electrical conductivity of the material [15]. These parameters are directly related to the electronic properties of the material and, for convenience, include power factor. The thermoelectric power factor characterizes the ability of a thermoelectric generator to generate electrical energy in an external circuit and is defined as:

$$P = \sigma\alpha^2.$$

3. RESULTS AND DISCUSSION

3.1. Surface Morphology and Crystal Structure of Mn_4Si_7 Thin Films

Figure 4 shows a 3*D* image of a manganese silicide nanofilm grown by magnetron sputtering, obtained using an atomic force microscope. The average roughness height of the HMS film is $r_z = 34.7$ nm, and the surface is completely covered with a peak. Figure 5 shows a 2*D* image of a Mn_4Si_7 nanofilm. Moreover, if we take images in only two dimensions, we see that we cannot easily discern differences in surfaces. The height of the islands is more visible in 3*D*. In both cases, evenly distributed waves are generated under the surface over large areas. This means that the thin surface layer is manganese silicide. AFM analysis shows that evidence of formation is a nanosize film obtained by the ion-plasma method. Figure 6 shows the formation profile of a manganese silicide nanofilm grown by the solid-phase ion plasma method in a

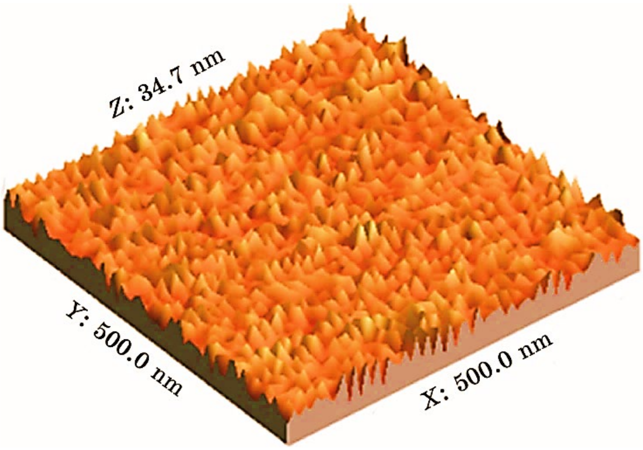

Fig. 4. 3*D* images of the surface of thin Mn_4Si_7 films obtained by atomic force microscopy.

magnetron sputtering device.

The qualitative composition of a thin film of manganese silicide, the crystal structure of the substance, as well as the arrangement of atoms in the unit cell have been determined. The texture of polycrystalline materials has been studied. In addition, the phase composition of the substance, phase diagrams, crystal sizes in the sample, radiation CuK_α (β-filter, Ni, $\lambda = 1.54178$ Å, current and voltage mode—30 mA, 40 kV) and constant rotation speed of the detector were assessed 0.05 degrees

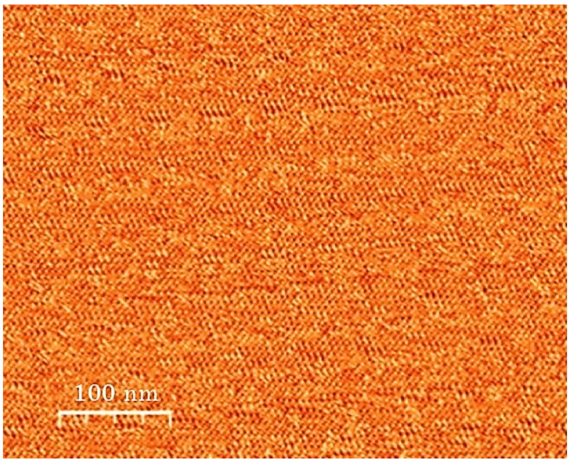

Fig. 5. 2*D* images of the surface of thin Mn_4Si_7 films obtained by atomic force microscopy.

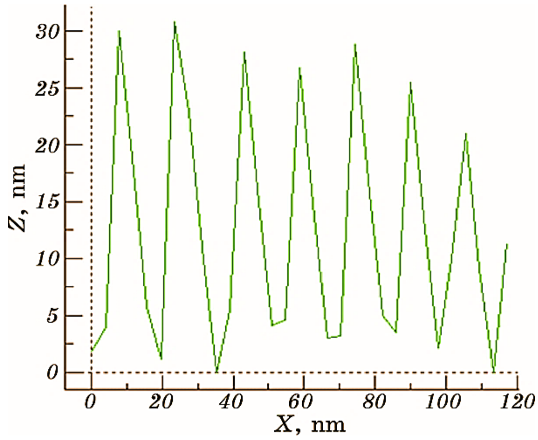

Fig. 6. Profile along the selected direction.

in steps of 4 degrees/min. The x-ray power was 2 kW. The results were analysed using a database. The penetration depth of radiation CuK_α is about 1 mm (980 μm) for light elements (carbon) and several microns for heavy elements (Ag, Pt). For most inorganic substances, CuK_α is tens of microns (μm) for simple compounds.

Figure 7 shows the spectral dependences obtained using the Mn_4Si_7 diffractometer method. In addition, Miller indices are given. We used the Rietveld method to refine the structure from x-ray data [9–11]. The principle of the method is to use independent intensity measurements at each point of the diffraction pattern to describe the line profile using analytical functions instead of using the integrated reflection intensity. Object parameters, including structural, hardware and other characteristics, are refined using the nonlinear least squares

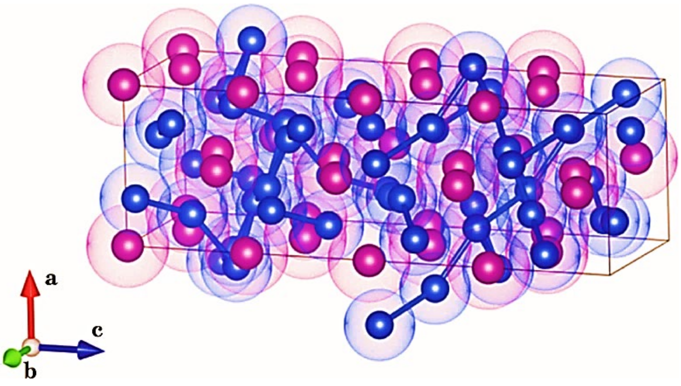

Fig. 7. Crystal structure (tetragonal structure, space group $Pm3m$).

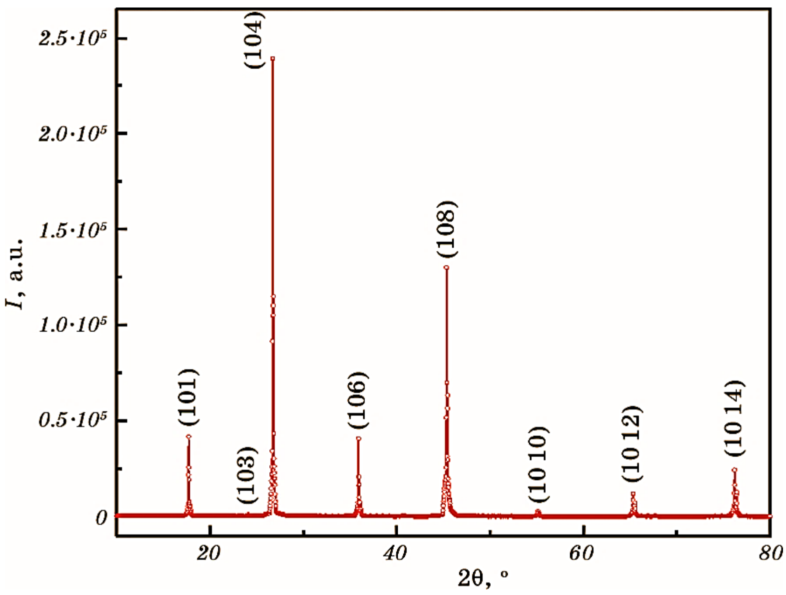

Fig. 8. X-ray diffraction pattern of Mn_4Si_7 crystal.

TABLE 1. Type and lattice parameters of silicide films.

Silicide	In this work	
	Grille type	Lattice parameters, Å
Si	Cubic	$a = 5.45$
$CoSi_2$ [5]	Cubic	$a = 5.40$
Mn_4Si_7	Tetragonal	$a = 5.7$, $c = 15.3$

method. Using this refinement method, we determined the Miller indices (*hkl*). As mentioned above, x-ray diffractometry of polycrystalline films allows quantitative elemental analysis.

Figure 8 shows x-ray diffraction analysis and spectral dependences of a thin film of manganese silicide. XRD analysis at room temperature shows that peaks 17.292, 27.412, 36.321, 45.842, 55.792, 65.247 and 77.634 are visible from several angles. The main ideal peak appears at an angle of 27.412 degrees (104).

When heated to 700 K, the angle of the peaks in the image does not change, but the intensity does. The release of some light volatile elements during heating and crystallization can be explained by the crystallization of the sample. The x-ray phase analysis method presented in the literature [12, 13] shows that in a sample heated to 800 K, x-ray phase analysis peaks appear at certain angles, although the peaks are very small in intensity and contrast.

3.2. Measurement of Electrophysical and Thermoelectric Properties of Samples

The electrical parameters of manganese silicide films of various thicknesses deposited on the surfaces of silicon and glass by the ion-plasma method in high vacuum were measured on an ECOPIA instrument (HMS-5000), and comparative data on the electrical parameters of thin Mn_4Si_7 coatings are presented (Table 2). Figure 9 shows the tempera-

TABLE 2. Mn_4Si_7 film deposited on glass (1), Mn_4Si_7 film deposited on silicon (2).

Measurements	Mn_4Si_7 coated on glass surface (1)	Mn_4Si_7 coated on silicone surface (2)
Resistivity, Ω·cm	$4.1678\cdot10^{-3}$	$1.2453\cdot10^{-3}$
Resistance, Ω	612	454
Average Hall coefficient, cm³/C	$5.7642\cdot10^{-2}$	$2.8979\cdot10^{-5}$
Conductivity, S/cm	239.94	802.99
Sheet concentration, cm⁻²	$3.2488\cdot10^{15}$	$2.2036\cdot10^{18}$
Bulk concentration, cm⁻³	$1.0829\cdot10^{20}$	$2.1541\cdot10^{23}$
Mobility, cm²/(V·s)	13.83	$2.327\cdot10^{-2}$
Sheet resistance, Ω/	138.93	121.74
A–C Hall coefficient, cm³/C	$1.4251\cdot10^{-1}$	$2.9439\cdot10^{-5}$
B–D Hall coefficient, cm³/C	$-2{,}7224\cdot10^{-2}$	$2.8519\cdot10^{-5}$
Ratio vertical/horizontal	0.77849	0.97469

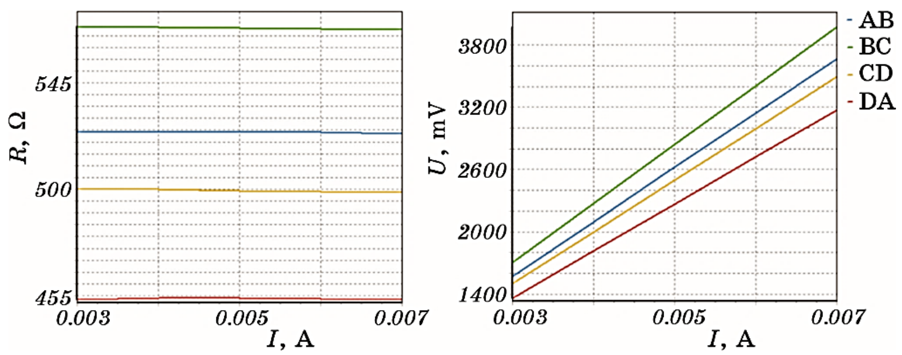

Fig. 9. Electrophysical parameters of Mn_4Si_7 thin films (resistance *vs.* current and *I–U* curve).

ture dependence of I–U curve and the electrical resistance of the samples.

The MnSi film deposited on a silicon substrate with a resistivity of 3–5 Ω·cm had an n-type and the Seebeck coefficient was close to −140 μV/K. The thickness of the films was about 146 nm. The resistance decreased with increasing temperature. However, the relationship between resistance and temperature was very complex due to the shrinkage effect of the substrate. The figures show the temperature dependences of the electrical conductivity and Seebeck coefficient of thin Mn_4Si_7 films of various thicknesses grown in ion-plasma oats (Fig. 10).

With increasing temperature, the resistivity first decreased from 124 to 118 mΩ·cm, increased slightly after 400 K, and then, sharply decreased. This behaviour indicates that Mn_4Si_7 is a semiconductor. Due to the average crystallinity of the film, the Seebeck coefficient was not very low.

The Seebeck coefficient of the film with an initial thickness of 172 nm was larger than that of sample-1, but the Seebeck coefficient increased faster after 560 K, which can be attributed to the crystallinity of the film thickness.

The resistivity of the sample deposited on the silicon surface was about 9.88 mΩ·cm at room temperature. With increasing temperature, the electrical conductivity increased slightly and then increased sharply above 530 K. The film was p-type at room temperature and n-type after 460 K. Near the Mn_4Si_7/Si interface, the silicon substrate heavily doped with manganese is n-type, and the donor state has separated from the conduction band with the energy level. We can say that $E_d = 0.354$ eV.

At temperatures above 580 K, the resist is thermally activated with apparent activation energy of 0.492 eV. If we take the activation ener-

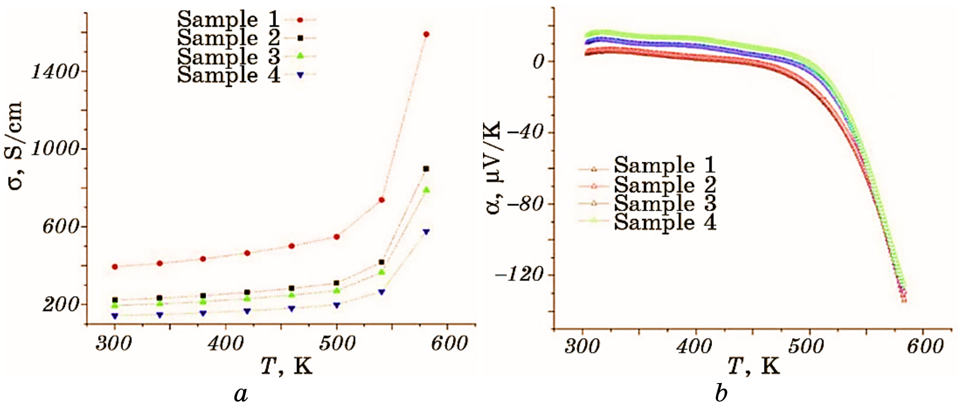

Fig. 10. Temperature dependence of electrical conductivity and Seebeck coefficients.

gy of the material in this intrinsic region to be half the forbidden energy gap, this indicates an estimated energy gap of about 0.984 eV:

$$E_g = E_g(0) \pm \beta\tau, \qquad (2)$$

where E_g is the energy band gap, T is the temperature, then the coefficient $\beta = dE_g/dT = -0.80 \cdot 10^{-4}$ eV/K [16]. The Seebeck coefficient is −1.32 μV/K at 300 K and −136 μV/K at 530 K, respectively. With increasing temperature, the concentration of electrons excited from the donor state to the conduction band increases. As a result, the Seebeck coefficient decreases and finally the sample changes from *p*-type to *n*-type. For the sample prepared by the ion plasma method, the band gap at room temperature was $E_g = 0.354$ eV, measured by the optical method.

Figure 11 shows the power factor as a function of temperature for samples of four different thicknesses. As a result of measurements, the power factor turned out to be small ($P \cong 1$–4 mW/(m·K^2)) and increased very little in the temperature range of 300–450 K and increased sharply in the range of 500–580 K ($P \cong 850$–3690 mW/(m·K^2)). As the thickness decreases, the power factor increases. Using the magnetron sputtering method, a Mn_4Si_7 film with a resistivity of $1.24 \cdot 10^{-3}$ Ω·cm was obtained at room temperature. The power factor reached 3684 μW/(m·K^2) at 575 K. Due to this high-power factor, the *n*-type HMS material can outperform the *p*-type HMS material in the development of thermoelectric generators.

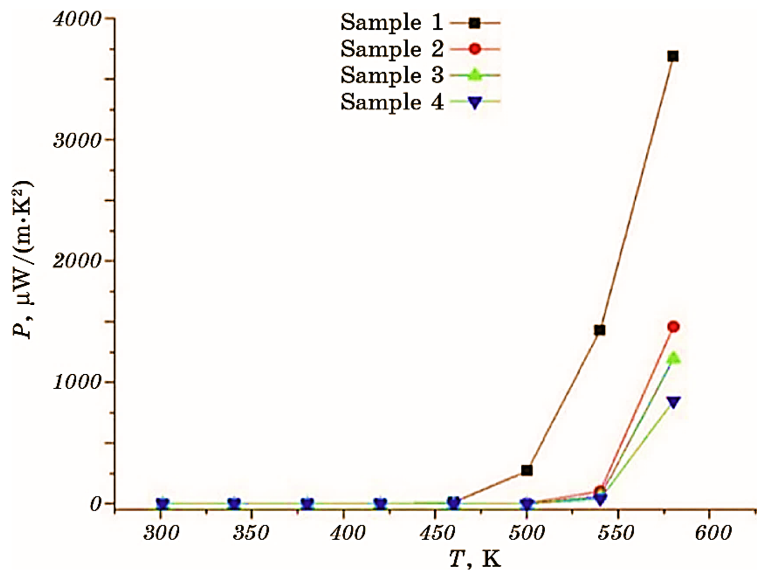

Fig. 11. Power factor dependence on temperature.

4. CONCLUSION

A film of high-manganese silicide of various thicknesses was grown on the surface of a silicon crystal in a magnetron sputtering installation using the solid-phase ion-plasma method. The surface morphology of Mn_4Si_7 crystals depending on their state was studied using a Quanta 200 3*D* microscope (Scios FEI). The electrical parameters of a thin layer of Mn_4Si_7 samples with a thickness of approximately 34.7–172 nm were studied on an ECOPIA device (HMS-5000). Structural analysis of the Mn_4Si_7 crystal was recorded on an XRD-6100 x-ray diffractometer; spectra were recorded at room temperature. Spectrogram peaks based on Miller indices and interplanar distances indicate newly formed manganese silicide compounds. As a result of the research, it was established that the electrical properties of Mn_4Si_7 coatings grown on the surface of glass and silicon by magnetron sputtering are higher on silicon. It has been established that when a Mn_4Si_7 nanocluster is heated and cooled, the Seebeck coefficient changes from −1.32 μV/K to −140 μV/K depending on the order of the nanolayer and the thickness of the coating, and the resistance of the coating decreases upward up to 1.5 times. As a result of the analysis of the measured thermoelectric properties, we concluded that the 'ion-plasma' method is a more effective method for producing high-quality thermoelectric materials. The resulting films can be used in sensors for IR and UV detectors.

REFERENCES

1. M. T. Normuradov, I. R. Bekpulatov, V. V. Loboda, B. D. Donaev, and I. Kh. Turapov, *J. Phys. Math.*, **16**: 78 (2023).
2. B. D. Igamov, G. T. Imanova, A. I. Kamardin, and I. R. Bekpulatov, *Bulletin of the Karaganda University. Series 'Physics'*, No. 3 (111): 50 (2023).
3. B. B. Pitarch, J. P. Gonjal, A. Powell, P. Ziolkowski, and J. G. Canadas, *J. Applied Phys.*, **124**, No. 2: 025105 (2018).
4. C. L. Shen, S. M. Yang, and K. C. Lu, *Nanomaterials*, **10**, Iss. 9: 1880 (2020).
5. K. T. Dovranov, M. T. Normuradov, Kh. T. Davranov, and I. R. Bekpulatov, *Ukrainian J. Phys.*, **69**, No. 1: 20 (2024).
6. D. Y. N. Truong, *Thermoelectric Properties of Higher Manganese Silicides* (Disser. for PhD in Chemistry) (Waterloo: 2015).
7. S. Choia, K. Kuboa, N. Uchiyamaa, and T. Takeuchi, *J. Alloys Compd.*, **921**: 166104 (2022).
8. Q. R. Hou, W. Zhao, Y. B. Chen, and Y. J. He, *Int. J. Modern Phys. B*, **23**, No. 16: 3331 (2009).
9. M. Yu. Tashmetov, F. K. Khallokov, N. B. Ismatov, I. I. Yuldashova, I. Nuritdinov, and S. Kh. Umarov, *Physica B: Cond. Matter*, **613**: 412879 (2021).
10. S. K. Umarov, I. Nuritdinov, Z. Z. Ashurov, and F. K. Khallokov, *Techn. Phys.*, **64**: 183 (2019).

11. M. T. Normuradov, Sh. T. Khozhiev, K. T. Dovranov, Kh. T. Davranov, M. A. Davlatov, and F. K. Khollokov, *Ukrainian J. Phys.*, **68**, No. 3: 210 (2023).
12. L. Smrcok, V. Langer, M. Halvarsson, and S. Ruppi, *J. Crystallography*, **216**, Iss. 7: 409 (2001).
13. K. Dovranov, M. Vinnichenko, A. Kodirov, M. Normuradov, M. Davlatov, J. Parmonov, Kh. Davranov, D. Nabiyev, and N. Kurbonov, *2024 Int. Conf. Electrical Eng. Photonics (EExPolytech) (Oct. 17–18, 2024)* (Saint Petersburg: 2024), p. 308.
14. I. V. Erofeeva, M. V. Dorokhin, V. P. Lesnikov, Yu. M. Kuznetsov, A. V. Zdoroveishchev, and E. A. Pitirimova, *XXI Int. Symp. 'Nanophysics and Nanoelectronics' (March 13–16, 2017)* (Nizhny Novgorod: 2017), p. 1403.
15. Q. R. Hou, W. Zhao, Y. B. Chen, D. Liang, X. Feng, H. Y. Zhang, and Y. J. He, *Appl. Phys. A*, **86**: 385 (2007).
16. Z. M. Wang, Q. R. Hou, and Y. J. He, *Appl. Phys. A*, **80**: 1807 (2005).